Phasor Analysis of Pulse Tube Refrigerator

L. Mohanta, M.D. Atrey
Department of Mechanical Engineering
Indian Institute of Technology Bombay, Powai
Mumbai-400076, India

ABSTRACT

A phasor diagram for a pulse tube refrigerator (PTR) is a vectorial representation of mass flow rate, pressure, and temperature at different locations as a function of time. With the help of a phasor diagram, the operation of different types of pulse tube refrigerators can be well understood. Phasor analysis based on these diagrams gives an idea regarding the underlying complex phenomena of the PTR. In the present work, a simplified model has been presented based on the assumption that there is no phase difference between temperature and pressure throughout the working space. The phasor analysis is extended to a two-stage Orifice Pulse Tube Refrigerator (OPTR) and to a Double Inlet PTR (DIPTR). The important contribution of the work is that it highlights the condition for which the DIPTR will work better than the OPTR.

INTRODUCTION

In recent years, pulse tube refrigerator (PTR) technology has undergone a lot of improvement. PTRs are now widely used for various applications, e.g. MRI, NMR, space technology, cooling of SQUIDS etc. This is due to the absence of cold moving part in PTRS, which improves their vibration characteristics and reliability. The PTR works in a cyclic manner which consists of a) Compression, b) Constant Pressure Regenerative cooling, c) Expansion and d) Constant pressure regenerative heating [1]. Different analyses have been presented in order to analyse the underlying phenomena taking place in the PTR. Various numerical models have been proposed that give quite good result [2, 3]. However, for a DIPTR or for a two-stage PTR, these analyses become more mathematical in nature and therefore are not easy to understand. Also, they do not help us to imagine the physical processes that are taking place in the PTR. In view of this, the present work highlights the working of different types of PTR using phasor analysis, which is a vectorial representation of the working of the PTR. Basic analysis of the PTR using phasor diagrams was introduced by Radebaugh [4], while Kittel et al. [5] carried out similar analyses using Taylor series approximation. Hofmann and Pan [1] explained the working of different types of PTR with phasor diagrams and analyzed them using an electrical analogy and complex geometry. A phasor diagram for a Double Inlet PTR was suggested by Chokhawala et al. [6].

In the present work, a detailed phasor analysis for a two-stage PTR, both OPTR and DIPTR, is presented based on the law of conservation of mass. The phasor analysis helps to understand the importance of phase difference between mass flow rate at the cold end and the pressure pulse in the pulse tube. The refrigerating effect for different types of PTR strongly depends on the

Cryocoolers 16, edited by S.D. Miller and R.G. Ross, Jr.

phase shift arrangement and also on the phase difference. Due to the complexities of the flow involved in the two-stage DIPTR and OPTR, the phasor diagram put forth in the present work will prove to be very helpful to understand the importance of these parameters. The present work also introduces the concept and importance of phase lead of the double inlet flow entry in the DIPTR. The analysis also comes out with a necessary condition on the value of the phase lead angle in order to make a DIPTR function better in terms of refrigerating effect, as compared to an OPTR

ANALYSIS FOR OPTR

Assumptions

a) The gas obeys the ideal gas law.
b) There is no phase difference between the pressure and the mass flow rate at the hot end through the orifice of the pulse tube.
c) There is no phase difference between the pressure and the temperature throughout the working space of the PTR.
d) The variation of pressure, temperature and mass flow at a given location is sinusoidal.
e) The pulse tube behaves adiabatically during the operation.

Pressure and Temperature Variations

In the pulse tube, pressure and temperature variations are given as:

$$P = P_0 + P_1 \cos(\omega t) \tag{1}$$

$$T = T_0 + T_1 \cos(\omega t) \tag{2}$$

Applying the adiabatic condition to the pulse tube,

$$\frac{T}{T_0} = \left(\frac{P}{P_0}\right)^{\frac{\gamma-1}{\gamma}} \tag{3}$$

Using Taylor series expansion and neglecting higher order terms [5],

$$\frac{T_1}{T_0} = \frac{\gamma-1}{\gamma}\frac{P_1}{P_0} \tag{4}$$

Mass Flow in the Pulse Tube

Considering the whole pulse tube as a control volume and applying the law of conservation of mass,

$$\frac{d\left(\rho V_{pt}\right)}{dt} = \left(\rho \dot{v}\right)_c - \left(\rho \dot{v}\right)_h \tag{5}$$

Assuming that the pulse tube is at a mean temperature, density can be taken as $\rho = \dfrac{P}{RT_{mpt}}$

$$\frac{d\left(PV_{pt}\right)}{RT_{mpt}dt} = \dot{m}_c - \dot{m}_h \tag{6}$$

$$\frac{V_{pt}}{RT_{mpt}}\frac{dP}{dt} = \dot{m}_c - \dot{m}_h \tag{7}$$

Mass flow rate at the hot end, $\dot{m}_h$, through orifice is directly proportional to pressure difference [5].

$$\Delta P = P_1 \cos \omega t \tag{8}$$

Mass flow rate at hot end is given as [5],

$$\dot{m}_h = \frac{T_h}{T_c} C_1 P_1 \cos \omega t \tag{9}$$

Combining Eq. (9) and Eq. (7),

$$\dot{m}_c = \frac{T_h}{T_c} C_1 P_1 \cos \omega t + \frac{\omega V_{pt}}{R T_{mpt}} P_1 \cos(\omega t + \pi/2) \tag{10}$$

From Eq (10), it is clear that mass flow rate at the cold end consists of two components. The first term in the right hand side is the contribution resulting from the mass flow rate at the hot end through the orifice which is in phase with the pressure. The second term represents the additional amount of mass entering the pulse tube due to pressurization, which is leading the earlier term by 90^o. Fig.1 shows the equivalent phasor representation of Eq. (10). The phase angle θ represents the phase difference between the pressure pulse and T $\dot{m}_c$ T. The numerical analysis of the first law of thermodynamics applied to the PTR also shows a similar phase difference in the mass flow rate at different locations of the pulse tube [7].

Enthalpy flow

Due to the pulsating nature of the flow in the pulse tube, time-averaged enthalpy is considered for energy balance for a cycle. Fig. 2 shows enthalpy flow in the pulse tube.

Applying the first law of thermodynamics to the cold end heat exchanger of the PTR as shown in Fig. 2 gives,

$$\dot{Q} = \langle \dot{H} \rangle - \langle \dot{H}_r \rangle \tag{11}$$

where Q is the refrigerating effect, $\langle \dot{H} \rangle$ is the time-averaged enthalpy from the cold end heat exchanger of the pulse tube and $\langle \dot{H}_r \rangle$ is the time-averaged enthalpy flow from regenerator to cold end heat exchanger.

For perfect regeneration, $\langle \dot{H}_r \rangle$ =0

Hence the refrigerating effect obtained will be,

$$\dot{Q} = \langle \dot{H} \rangle = \frac{C_p}{\tau} \int_0^\tau \dot{m}_c T dt \tag{12}$$

Substituting the expression for mass flow rate from Eq. (10) and using Eq. (3),

$$\langle \dot{H} \rangle = \frac{C_p}{\tau} \int_0^\tau (\dot{m}_c)(T_c + T_1 \cos \omega t) dt \tag{13}$$

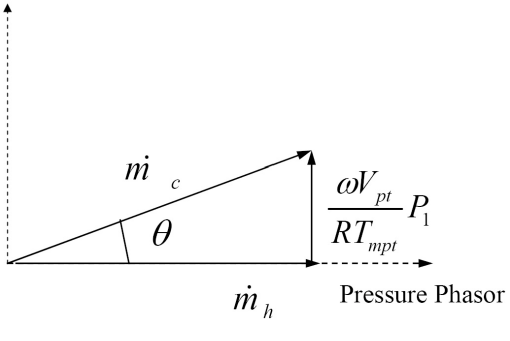

Figure 1. Phasor diagram showing mass flow rate at hot end and cold end of pulse tube.

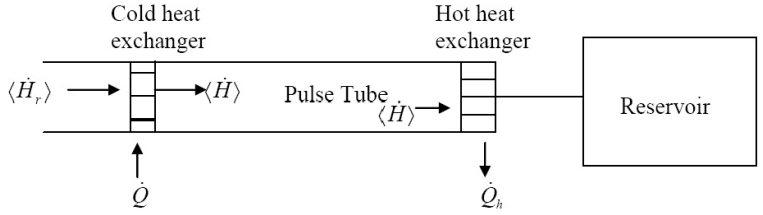

Figure 2. Enthalpy flow in the pulse tube.

The integration of the second term in Eq. (10) becomes zero as this term is 90^0 out of phase. This shows there is no contribution to the refrigerating effect by the mass flow due to pressurization. Hence Eq. (13) reduces to

$$\langle \dot{H} \rangle = \frac{C_p}{\tau} \int_0^{\tau} \frac{T_h}{T_c} C_1 P_1 \cos \omega t * (T_c + T_1 \cos \omega t) dt \tag{14}$$

On further integration,

$$\langle \dot{H} \rangle = \frac{C_p}{5} \frac{P_1^2}{P_0} T_h C_1 \tag{15}$$

This can be expressed in terms of mass flow rate at the cold end, $\dot{m}_c$. From Fig.1 $\dot{m}_h$ and $\dot{m}_c$ can be related as follows.

$$\cos\theta = \frac{|\dot{m}_h|}{|\dot{m}_c|} \text{ And } Q = \langle \dot{H} \rangle = \frac{1}{2} R T_c \frac{P_1}{P_0} |\dot{m}_c| \cos\theta \tag{16}$$

This result is in agreement with Radebaugh [4] and Kittel [5]. Eqs. (15), (16) show that the smaller is the phase difference, θ , and larger is the mass flow rate, $\dot{m}_c$, and the more refrigerating effect will be obtained. In other words, the product $\dot{m}_c \cos\theta$ has to be as large as possible.

In the case of BPTR, the mass flow rate at the hot end ($\dot{m}_h$) is zero, which implies θ is equal to 90^0. Hence, theoretically, the refrigerating effect should be equal to zero for this configuration. However, due to heat transfer from gas to the wall of the pulse tube, θ decreases slightly below 90^0. The numerical value of θ could also be indicative of the losses in the system. As the loss increases, θ increases and that will lead to decrease in the refrigerating effect.

PHASOR DIAGRAM FOR TWO STAGE OPTR

The phasor diagram for a two-stage OPTR can be drawn in a similar fashion as that of the single-stage OPTR. For the two-stage PTR, both the pulse tubes are considered separately. Fig. 3 shows the phasor diagram for both stages of the pulse tube. Fig. 3(a) gives the phasor diagram for the second stage pulse tube of the two-stage OPTR where $\dot{m}_{h2}$ and $\dot{m}_{c2}$ represent the phasors for mass flow rate at the second stage hot and cold ends, respectively. It can be seen

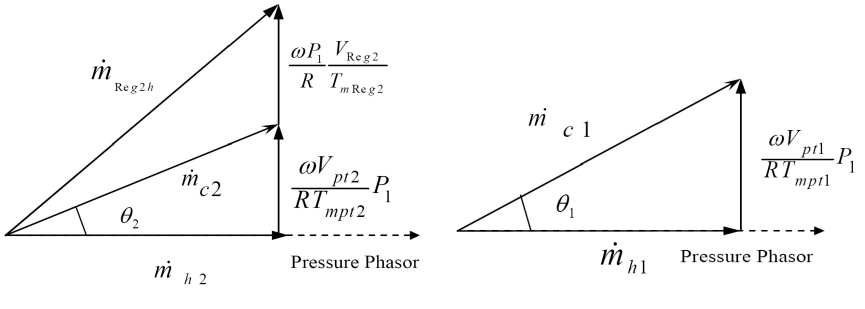

Figure 3. Phasor diagram for pulse tube (a) Second stage (b) First stage.

from Fig. 3(a) that the $\dot{m}_{\text{Reg2}h}$, phasor for mass flow rate at the hot end of the second stage regenerator, can be obtained by adding the phasor for regenerator-2 loss, ($\frac{\omega P_1}{R}\frac{V_{\text{Reg2}}}{T_{m\text{Reg2}}}$), to the phasor for mass flow rate at the cold end of the pulse tube-2, $\dot{m}_{c2}$ Fig. 3(b) gives the phasor diagram for the first stage of the two stage OPTR. The flow coming out of regenerator-1 gets divided into two streams; one stream goes to the first stage pulse tube and the second one goes through regenerator-2. Therefore, the mass flow rate through the cold end of the regenerator-1 ($\dot{m}_{\text{Reg1}c}$) can be obtained by adding the phasors $\dot{m}_{c1}$ and $\dot{m}_{\text{Reg2}h}$ as given in Eq. (17).

$$\dot{m}_{\text{Reg1}c} = \dot{m}_{\text{Reg2}h} + \dot{m}_{c1} \tag{17}$$

Redefining $\dot{m}_{c1}$ as given in Eq. (10) for the first stage,

$$\dot{m}_{c1} = \frac{T_h}{T_{c1}} C_1 P_1 \cos(\omega t) + \frac{\omega V_{pt1}}{RT_{mpt1}} P_1 \cos(\omega t + \pi/2) \tag{18}$$

As shown in Fig. (3), $\dot{m}_{\text{Reg2}h}$ can be expressed as,

$$\dot{m}_{\text{Reg2}h} = \frac{T_h}{T_{c2}} C_1 P_1 \cos\omega t + \frac{\omega V_{pt2}}{RT_{mpt2}} P_1 \cos(\omega t + \pi/2) + \frac{\omega}{R}\frac{V_{\text{Reg2}}}{T_{m\text{Reg2}}} P_1(\omega t + \pi/2) \tag{19}$$

Fig. 4 shows the combined phasor diagram for the two-stage OPTR including the losses in the compressor. The effect of void volume in the heat exchangers is neglected. The refrigerating effect (Q) can be calculated as earlier using Eq. (15) or (16) separately for both the stages.

ANALYSIS FOR DIPTR

The analysis for the OPTR provides the background for the analysis for the DIPTR. A DIPTR differs from an OPTR by a connection from the high pressure line to the hot end of the pulse tube as shown in Fig. 5. All the assumptions are the same as those for the OPTR. In addition, a phase lead angle, α is considered between the flow through double inlet valve and the pressure pulse in the PTR.

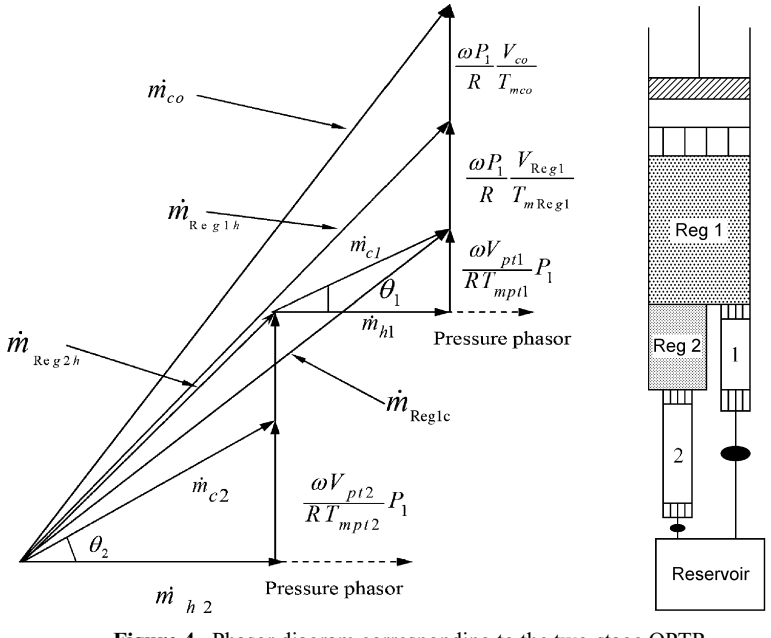

Figure 4. Phasor diagram corresponding to the two-stage OPTR.

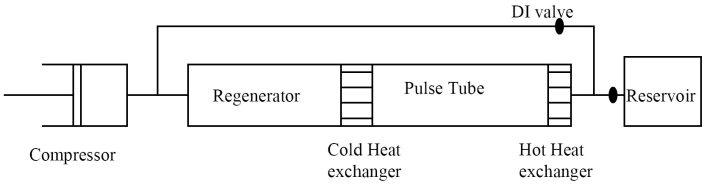

Figure 5. Schematic diagram of Double Inlet Pulse Tube Refrigerator (DIPTR).

Mass Flow in the Pulse Tube (DIPTR)

Considering the whole pulse tube as a control volume and applying the law of conservation of mass,

$$\frac{d\left(\rho V_{pt}\right)}{dt} = \left(\rho \dot{v}\right)_c - \left(\rho \dot{v}\right)_o + \left(\rho \dot{v}\right)_{DI} \tag{20}$$

$$\frac{d\left(PV_{pt}\right)}{RT_{mpt}\,dt} = \dot{m}_c - \dot{m}_o + \dot{m}_{DI} \tag{21}$$

$$\dot{m}_h = \dot{m}_o - \dot{m}_{DI} \tag{22}$$

where $\dot{m}_h$ is the net mass flow rate leaving the hot end of the pulse tube.

$$\frac{d\left(PV_{pt}\right)}{RT_{mpt}\,dt} = \dot{m}_c - \dot{m}_h \tag{23}$$

Thus, $\dot{m}_o$ and $\dot{m}_{DI}$ are directly proportional to the pressure difference across the valve. As per the assumption, $\dot{m}_{DI}$ leads the pressure by phase angle α. Substituting $\dot{m}_h$ in Eq. (23) in terms of pressure we get,

$$\dot{m}_c = \frac{T_h}{T_c} C_1 P_1 \cos\omega t + \frac{\omega V_{pt}}{RT_{mpt}} P_1 \cos(\omega t + \pi/2) - \frac{T_h}{T_c} C_2 P_1 \cos(\omega t + \alpha) \tag{24}$$

Figs. 6 (a) and (b) show the equivalent representation of the expression given in Eq. (24) in terms of phasors. It can be seen from these figures that $\dot{m}_h$ depends on $\dot{m}_o$ and $\dot{m}_{DI}$ which are controlled by the respective valve openings. Fig. 6 (a) shows the phasor diagram when the DI phase lead angle α is less than 90^0, while Fig. 6(b) shows the phasor diagram when α is greater than 90^0. It can be seen from these figures that $\dot{m}_c \cos\theta$ is more than $\dot{m}_o$ when α is more than 90°.

Enthalpy Flow

Substituting the mass flow rate expression from Eq. (24) for calculating refrigerating effect,

$$\langle \dot{H} \rangle = \frac{C_p}{\tau}\left[\int_0^{\tau} \frac{T_h}{T_c} C_1 P_1 \cos\omega t * (T_c + T_1 \cos\omega t)dt - \int_0^{\tau} \frac{T_h}{T_c} C_2 P_1 \cos(\omega t + \alpha) * (T_c + T_1 \cos\omega t)dt\right] \tag{25}$$

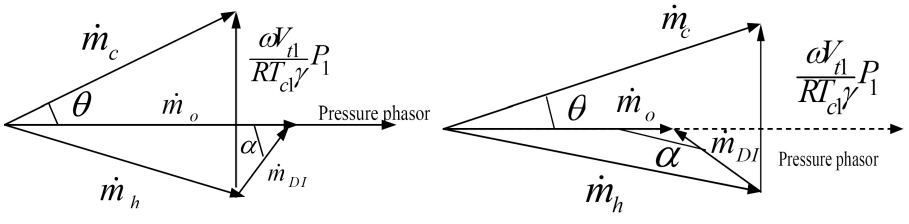

Figure 6. Phasor diagram for DIPTR when phase lead (a) less than 90^o (b) more than 90^o

$$\Rightarrow Q_{DIPTR} = \langle \dot{H} \rangle = \frac{C_p}{5}\frac{P_1^2}{P_0}T_h C_1 - \frac{C_p}{5}\frac{P_1^2}{P_0}T_h C_2 \cos\alpha \tag{26}$$

Eq. (26) shows that the refrigerating effect for the DIPTR depends on α. The first term is the same as that for the OPTR, while the second term represents the contribution due to the flow through the DI valve.

From Fig. 6 we can rewrite the Eq. (26) as,

$$Q_{DIPTR} = \frac{1}{2} R T_c \frac{P_1}{P_o} |\dot{m}_c| \cos\theta \tag{27}$$

Eq. (27) indicates the fact that for maximum Q_{DIPTR}, $\dot{m}_c \cos\theta$ has to be as large as possible.

PHASOR DIAGRAM FOR TWO STAGE DIPTR

The phasor diagram can be drawn for a two-stage DIPTR by considering two pulse tubes separately and finally adding them together as done in the earlier case for the two-stage OPTR. Fig. 7 shows the phasor diagram for the two-stage DIPTR. The mass flow rate through regenerator-1 ($\dot{m}_{\mathrm{Reg1}c}$) is divided through pulse tube-1 and regenerator-2 which is given below,

$$\dot{m}_{\mathrm{Reg1}c} = \dot{m}_{\mathrm{Reg2}h} + \dot{m}_{c1} \tag{28}$$

The mass flow rate at the cold end of the pulse tube-1 $\dot{m}_{c1}$ can be redefined from Eq (24), while $\dot{m}_{\mathrm{Reg2}h}$ is given as,

$$\dot{m}_{\mathrm{Reg2}h} = \frac{T_h}{T_{c2}} C_1 P_1 \cos\omega t + \frac{\omega V_{pt2}}{R T_{mpt2}} P_1 \cos(\omega t + \pi/2) - \frac{T_h}{T_{c2}} C_2 P_1 \cos(\omega t + \alpha) + \frac{\omega}{R}\frac{V_{\mathrm{Reg2}}}{T_{m\mathrm{Reg2}}} P_1 (\omega t + \pi/2) \tag{29}$$

The refrigerating effect for both the stages can be calculated separately using Eq. (26).

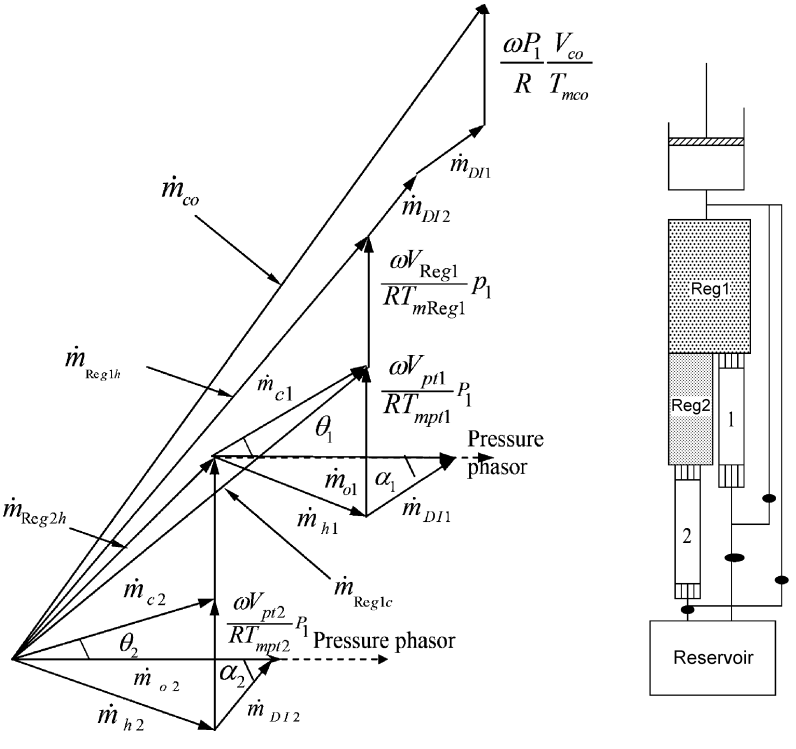

Figure 7. Phasor diagram corresponding to the two-stage DIPTR.

RESULTS AND DISCUSSION

Double Inlet Phase Lead Angle, α

From Eq. (26) and the phasor diagrams given in Fig.6, it can be seen that Q_{DIPTR} depends on the value of α when compared with Q_{OPTR} . It can be observed from Eq. (26) that α has to be more than 90° to achieve higher Q_{DIPTR} compared to $Q_{OPTR,}$ for the same opening of orifice. The value of α can be varied in practice by varying the opening of the double inlet valve. From Fig. 6 it can be noted that the projection of $\dot{m}_c$ on the pressure phasor, that is $\dot{m}_c \cos\theta$, increases with increase in α. When the double-inlet valve is closed, $\dot{m}_{DI}$ is equal to zero, and the expression for the QDIPTR given by Eq. (26) reduces to Eq. (15), which corresponds to an OPTR. As the value of α increase, the value of θ decreases, and the refrigerating effect increases. This fact is explained in detail in the next section.

Phasor Analysis for an Existing Single-Stage PTR

The above analysis is now applied to an existing PTR [8]. The flow coefficient for orifice and DIPTR valves are taken as given below.

C_1=6E-10kg/sec.pa [1, 9]
C_2=1E-10kg/sec.pa [1, 9]

Fig. 8 shows the variation of refrigerating effect (Q) with pressure ratio for different configurations of the PTR. Based on arguments made above, it can be seen that Q_{DIPTR} is less as compared to Q_{OPTR} when α is 45º (less than 90º) and more when it is 135º (more than 90º). Also, it can be seen from these figures that an increase in pressure ratio increases the refrigerating effect.

The variation of $\dot{m}_h$ and $\dot{m}_c$ with α is shown in the Fig. 9. At α equal to zero, although $\dot{m}_c$ is quite large, Q_{DIPTR} is minimum due to the fact that θ is also large for this case. It can be observed from Eq. (27) that, Q_{DIPTR} depends on the product of $\dot{m}_c$ and $\cos\theta$. This can also be confirmed from Fig. 6 that θ is maximum for α equal to zero, amounting to minimum Q_{DIPTR}.

Fig.10 shows the variation of Q_{DIPTR} and θ_{DIPTR} with α and Q_{OPTR} is plotted on the graph for comparison. As α increases from zero onwards, $\dot{m}_c$ decreases up to a certain value, but $\dot{m}_c \cos\theta$ increases continuously due to a decrease in θ. As a result, the refrigerating effect Q_{DIPTR} increases. At α equal to 90°, the value of $\dot{m}_c \cos\theta$ for the DIPTR is the same with or without the presence of $\dot{m}_{DI}$. In this case, Q_{DIPTR} with $\dot{m}_{DI}$ is the same as Q_{OPTR} ($\dot{m}_{DI}$ =0). This can be seen

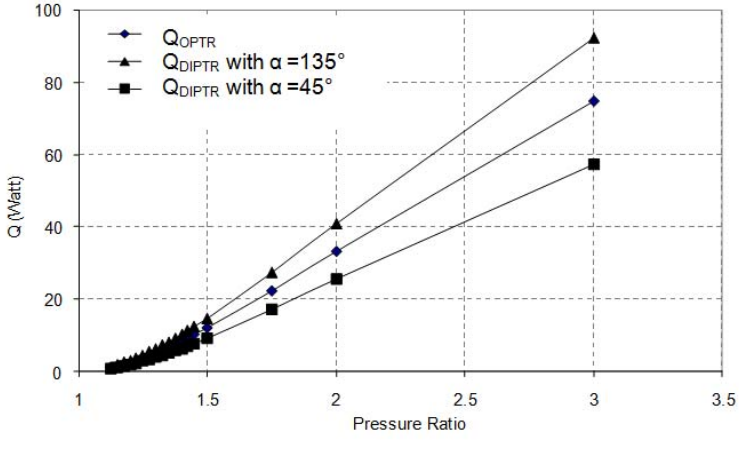

Figure 8. Variation of refrigerating effect with pressure ratio for different double inlet entry.

from Fig. 6. The presence of $\dot{m}_{DI}$ results in less gas passing through the regenerator, which causes $\dot{m}_c$ to be smaller and for θ_{DIPTR} to be reduced. In the absence of $\dot{m}_{DI}$, the value of $\dot{m}_c$ increases along with an increase in value of θ, which causes more losses in reality. Fig. 9 shows that, as the value of α increases in DIPTR, the phase difference θ reduces up to a certain minimum value and then increases. As discussed earlier, Q_{DIPTR} will be more comparable to Q_{OPTR} when α is greater than 90°. From Figs. 9 and 10, it can be seen that Q_{DIPTR} is maximum when α is 180°.

CONCLUSION

The present work highlights the fundamental relationship between mass flow rates at the hot and cold ends of the pulse tube and also the mass flow rate through the orifice and DI valve. Mass flow rate and enthalpy are expressed in terms of pressure, temperature, and harmonic terms. The work concludes that the phase difference, α and θ, are important parameters in estimating mass flow rates and refrigerating effect. The phasor diagrams have been presented for two-stage OPTR and DIPTR from which the concept of phase difference θ and DI phase lead angle α can be very well understood. It has been found that the refrigerating effect is directly proportional to the mass flow rate at the cold end and the amplitude of dynamic pressure. Also,

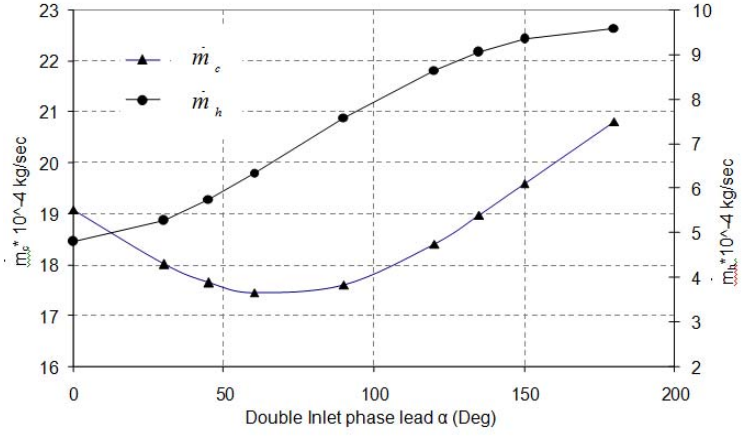

Figure 9. Variation of mass flow at hot and cold end of the pulse tube with phase lead angle.

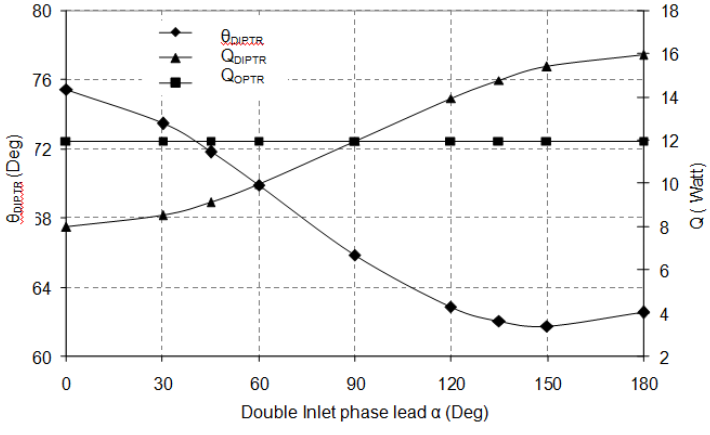

Figure 10. Variation of phase angle and refrigerating effect of DIPTR with phase lead angle.

for the DIPTR, the refrigerating effect will be more than for the OPTR when the DI phase lead angle α is greater than 90º. The phase diagrams presented for two-stage OPTR and DIPTR systems provide an insight into the physical phenomena taking place in these PTRs.

REFERENCES

1. Hofmann A, Pan H, "Phase shifting in pulse tube refrigerators," *Cryogenics* (1999), 39 (6), pp. 529-537.
2. Zhu S, Matsubara Y, "Numerical method of inertance tube pulse tube refrigerator," *Cryogenics* (2004), 44 (9), pp. 649-660.
3. Wang C, Wu PY and Chen ZQ, "Numerical analysis of double-inlet pulse tube refrigerator," *Cryogenics* (1993), 33 (5), pp. 526-530.
4. Radebaugh R. "A Review of pulse tube refrigeration," *Advances in Cryogenic Engineering,* 35 (1990), pp. 1191-1205.
5. Kittel P, Kashani A, Lee J M and Roach P R, "General Pulse Tube Theory," *Cryogenics* (1996) 36 (10), pp. 849-857.
6. Chokhawala M D, Desai K P, Barik H B, Narayankhedkar KG, Phasor analysis for double inlet pulse tube cryocooler," *Advances in Cryogenic Engineering* , 45 (2000), pp. 159-165.
7. He Y L, Huang J, Zhao C F, Liu Y W, "First and second law analysis of pulse tube refrigerator," *Applied Thermal Engineering*, 26 (2006), pp. 2301–2307.
8. Gawli BS, *Design and development of miniature pulse tube nitrogen liquefier*, PhD thesis, IIT Bombay, India.
9. Boer PCT, "Performance of the inertance pulse tube," *Cryogenics* (2002), 42 (3-4), pp. 209-221.